Journal of Computers Vol. 32 No. 1, 2021, pp. 11-26
doi:10.3966/199115992021023201002

2D Phase Unwrapping Method Based on Minimum Balanced Trees of Dual Residues

Jian Gao[1,3*], Rui Cheng[2], Yi-Xiang Chen[1,3], Chang Jiang[1,3]

[1] Department of Geographic Information, Nanjing University of Posts and Telecommunications, Nanjing, China
{gaoj,chenyixiang,jiangc}@njupt.edu.cn

[2] College of Telecommunications & Information Engineering, Nanjing University of Posts and Telecommunications, Nanjing, China
chengrui1825@126.com

[3] Smart Health Big Data Analysis and Location Services Engineering Lab of Jiangsu Province, Nanjing China

Received 25 October 2019; Revised 12 March 2020; Accepted 13 April 2020

Abstract. Phase unwrapping (PU) is an essential procedure in Interferometric Synthetic Aperture Radar (InSAR) and has been studied for decades. The advancement of sensors and platforms has made high-resolution InSAR available, at the same time, and has brought challenges to relative data processing. High-resolution data brings richer details, which could imply massive interference phase discontinuity. Traditional unwrapping methods designed for low- or medium-resolution low-scale data are usually difficult to obtain reliable unwrapping results. How to improve the reliability of wrapped phase data is critical in the design of unwrapping schemes. In this paper, a novel Minimum Balanced Trees (MBT) unwrapping strategy based on comprehensive reliability is presented. The MBT are designed to reconstruct phase discontinuity boundaries with minimum reliability residue pairs, which takes a combined reliability measure of residue distance and phase continuity. Dual residue points of each pair are connected by a line that is expected to be with a weighted minimum L^0 norm and is an ideal candidate for the discontinuity boundary. The MBT scheme includes solving eikonal equations, searching for minimum reliability pairs, and spanning detected trees. Most residue points would be covered and organized dynamically. Moreover, for the few uncoupled residues, we employ Flood-Filling on the priority map during path integration. All these procedures can be implemented to run in parallel mode, and the proposed method provides a robust and efficient option for PU, whose advantages are demonstrated in PU experiments on real InSAR wrapped phase data.

Keywords: phase unwrapping, minimum reliability residue pair, Minimum Balanced Trees (MBT), reliability map

1 Introduction

Interferometric Synthetic Aperture Radar (InSAR) is a critical Earth observation technology that has been developed for decades. With the advancement of sensor-related technologies and observation methods, InSAR data observation technology is promoted. SAR data with shorter observation periods and higher resolution could be available. That also brings new challenges to InSAR data processing. For example, higher spatial resolution in the acquisition of sampling data, due to range imaging, would make overlapping and upside-down problems are more evident and severe. The corresponding interferometric phase is more likely with discontinuity boundaries, which undoubtedly poses critical difficulty to Phase Unwrapping (PU) [1] that is a vital part of the InSAR interferometry process.

* Corresponding Author

PU retrieves absolute phase values from ambiguous ones modulo 2π, to reconstruct 3D information of observed targets. The main ideas of PU algorithms are based on an assumption of Nyquist's theorem that the phase differences between neighbor sampling data are less than half a cycle. With this assumption, the difference values can be obtained precisely by using the wrapping function. The absolute phase value of a point can be restored by integrating differences along a reliable path from a given reference position. The difficulty is that the assumption is untenable under some circumstances, likely where there is heavily undulating terrain or systematic noises are present. In such cases, the PU problem is ill-posed, and the neighbor phase difference would be more than half a cycle, meaning that the unique values cannot be specified directly. Compared to the normal wrapped range, differences higher than half a cycle bring about phase jumping in the defined 2D domain, just like rips on a continuous surface. Residues in the wrapped phase field can verify the existence of these rips (phase discontinuity boundaries). PU works mainly by direct or indirect detection and identification of reliable paths for unwrapping integration, with additional auxiliary constraints, which are expected to suppress abnormal neighbor phase differences.

Existing PU methods are based on different principles. Two main kinds of information are usually considered in PU schemes, wrapped phase residue points, and continuity statistics. The former are located at particular discrete positions on discontinuity boundaries, and the latter are indicators of phase data quality, they play a vital role in most PU methods. The classic branch-cut method [2] aims at connecting residue points to form discontinuity boundaries, complying with rules such as shortest distances. For the large-scale PU, tiling strategies [3-6] based on residue clustering have recently been provided with a designed convex hull algorithm for more effective schemes. The branch-cut method is even applied in parallel mode [7] to achieve higher operational efficiency with large data sets. On the other hand, continuity statistics work more indirectly. They are used as weights in minimum-norm methods, tuning the optimization criterion [8-10]. Based on statistical priority, the quality map-guided unwrapping method frequently appears in the research literature. Recently, new schemes have been proposed, such as frequency estimation [11], priority queuing on quantized quality maps [12-15], the grey-level co-occurrence matrix [16], Markov random fields [17], Kalman filtering [18], quality mapping with edges and shadow areas [19], quality-guided and surface-fitting [20], and even machine learning algorithms are taken to distinguish discontinuous features [21].

The two types of useful information, phase residues and data continuity, are both valuable for identifying phase discontinuity boundaries, and they are generally used separately in different methods. A better strategy is to combine the two, which is considered in methods such as branch-cuts based on edge detection from quality maps [22-23]. Another classic example is the network-flow based on graph theory, including Minimum Spanning Tree (MST), Minimum Cost Flow (MCF) [24] and Statistical-Cost Network-Flow Algorithm for Phase Unwrapping (SNAPHU) [25], focuses on constructing and optimizing a network. The network-optimizing methods with a minimum norm achieve more reliable results. The method is employed for time series data [26]. However, their actual performance is usually subject to the number of residues for iterative evolution, such as the simplex solving in SNAPHU, and that is more obvious for large-scale data.

In the paper, we proposed a novel PU method based on dual pairs with minimum reliability, which are designed to trace discontinuous phase boundaries. In the following sections, we introduce the proposed method, similar to the MST method, which adopts a network-constructing strategy but with some differences. Firstly, the basic units of trees are residue pairs which could keep the trees balanced always. Secondly, we provide a more reliable residue coupling method, based on their dual influencing regions of reliability. Finally, the residues are automatically assigned to different local pairs to construct local balance trees, which makes the method more natural to work in parallel and improve efficiency.

2 Principle and Method

To find reliable integration paths for unwrapping, the core idea of most PU methods focuses on detecting and shielding phase discontinuity boundaries directly or indirectly. Location information about residue points and low-quality phase is the most crucial point of the work. Based on the reliability of phase, we introduce a new way to reconstruct phase discontinuity boundaries with Minimum Balanced Trees (MBT).

2.1 Minimum Reliability Residue Pairs and Balanced Trees

With given phase quality weights Q in a 2D continuous domain, we define the reliability mark P of at (x, y) considering a nearby residue point S, as

$$P_S(x,y) = \int_c Q(u,v)\,\mathrm{d}s, \tag{1}$$

where $Q(u, v)$ refers to weight at (u, v) on c, s refers to an arc length of c, and c refers to a unique path from S, which minimizes the integration. At (x, y), reliability P_+ referencing to positive residues and reliability P_- referencing to negative ones are defined as

$$\begin{aligned} P_+(x,y) &= \min\{P_S(x,y) \mid S \in R_+\} \\ P_-(x,y) &= \min\{P_S(x,y) \mid S \in R_-\} \end{aligned},$$

where R_+ and R_- refer to the positive and negative residue sets, respectively. The sum of P_+ and P_- gives total reliability

$$P(x,y) = P_+(x,y) + P_-(x,y). \tag{2}$$

Phase reliability P_+, P_-, and P provide different comprehensive reliability descriptions of phase data. If a point has a low-reliability value, the point should be near to a residue, or in a noisy area, which suggests that it may be located on a discontinuity boundary.

During the reliability calculating, if the referencing point of P_-^a at positive residue point S_a, is located at negative residue point S_b, and vice versa, the referencing point of P_+^b is at S_a, we call the residues S_a and S_b a minimum reliability residue pair. The residues of a pair both have minimum reliability values referenced from each other, and their connecting line, $\mathbf{c}(S_a, S_b)$, with a direction from the positive residue to the negative, has the minimum reliability. That is

$$\mathbf{c}(S_a,S_b) = \arg\min_{\mathbf{c}}\left\{\int_{\mathbf{c}} Q(u,v)\,\mathrm{d}\mathbf{s} \,\middle|\, \mathbf{c}: S_a \to S_b\right\}. \tag{3}$$

Because the reliability is a minimum, the connecting lines for the residue pairs are inclined to be phase discontinuity boundaries. If residue pairs are detected and their corresponding connecting lines are specified according to (3), the obtained discontinuity boundaries would determine the unwrapping result. A PU optimization problem is based on minimum reliability residue pairs, but that is an NP-hard problem. Here we provide a scheme, MBT, based on minimum reliability residue pairs.

2.2 Constructing MBT with Dual Phase Residues

The MBT consist of minimum reliability residue pairs, and the construction process mainly includes searching for dual residues and merging them. In the beginning, we detect the minimum reliability residue pairs according to the definition, and they are taken as original MBT with only single-cycle directed phase jumps. Many residue pairs have different overlapping forms in the case of multi-cycle jumps. The lines connecting minimum residue pairs detected produce specific discontinuity boundaries. The discontinuity boundaries would be zero-weight, acting as superconductors, during flowing searching according to L^0 norm features.

The newly found residue pairs form new trees or are merged into old MBT. Such pair combinations bring about some exciting features. If connecting lines were in the same direction, an overlap would increase the cycle jump and span the old tree. However, an overlap with different directions would decrease the cycle jump and may split the old tree.

A simple example of constructing MBT is shown in Fig. 1. There are five positive and five negative residues shown as in (a). Here we evaluate the phase reliability with a constant weight for simplicity, positive residues' influencing regions, wherein reliabilities reference from them, are separated by solid lines and negatives' by dashed lines. According to the definition, residues of a minimum reliability residue pair would be at an intersection of their influencing regions. The detected four pairs are marked in grey areas, as shown in (b), and their directed connecting lines from positive residues to negative in (c) indicate single-cycle phase jumps. The remaining two residues in (c) make a residue pair, and their connecting line is not straight on account of the detected superconductive connecting lines. The

connecting line of the last pair is in the same direction as the old one, and the overlapping would increase the phase cycle shown as in (d). However, when the overlap is with different directions, shown as in (e), the combination would decrease the phase cycle, which may change the old connecting lines as in (f).

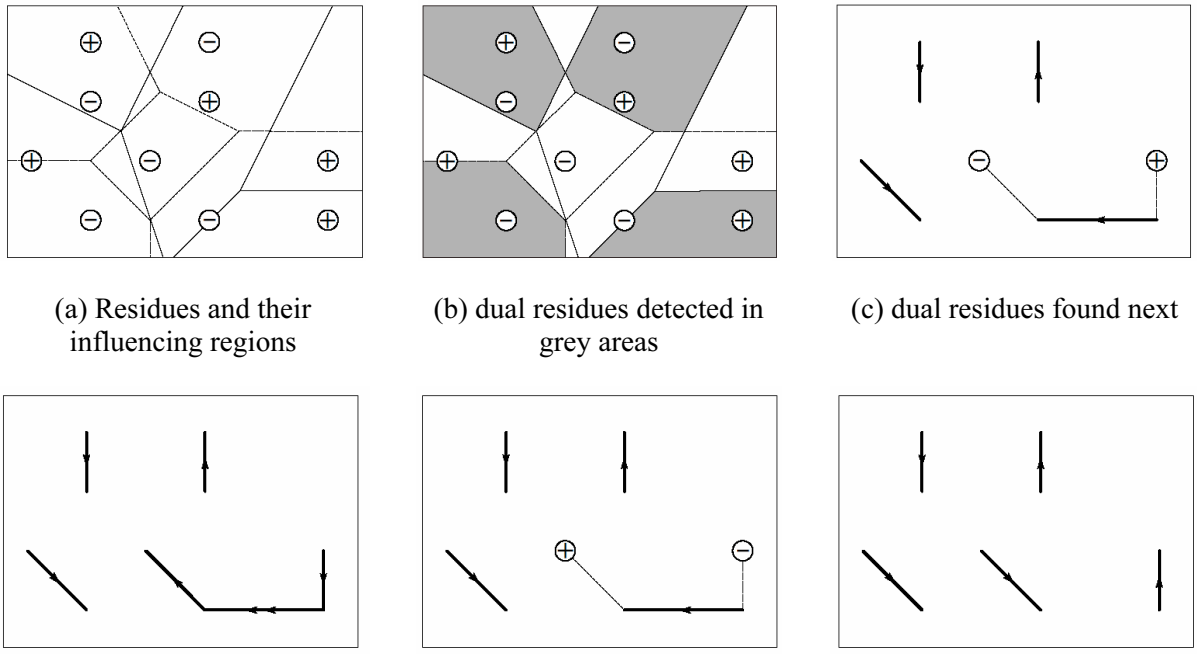

(a) Residues and their influencing regions

(b) dual residues detected in grey areas

(c) dual residues found next

(d) their combination

(e) a little change

(f) a different result

Fig. 1. Constructing MBT with minimum reliability residue pairs

The pair combinations will renew the MBT iteratively when new pairs are detected and added in until no more detectable. The added pairs produce expansions or decompositions of connecting lines, and each part is always residue balanced. Under ideal conditions, the MBT would cover all residues for a PU problem. However, it is not always like that, for example, when the residues are outside the defined domain. The potential residues outside must be considered during the detection of residue pairs. We regard the defined domain borders Ω as a set of candidate residues outside. The definitions of positive and negative reliability are rewritten as

$$P_{+}(x,y) = \min\{P_S(x,y) \mid S \in R_{+} \cup \Omega\}$$
$$P_{-}(x,y) = \min\{P_S(x,y) \mid S \in R_{-} \cup \Omega\}$$

The value of total reliability P on pair connecting lines is expected to be constant and equal to the minimum value of (3). However, that may not hold while potential residues on borders are involved. For example, positive residue A and negative residue B near border Ω, are shown in part (a) of Fig. 2, and their influencing regions are separated by solid and dashed lines, respectively. Total reliability P on two candidate connecting lines are shown in Fig. 2(b), and its value is not constant on the connecting line. In any case, the connecting lines of Ω−A and A−B should be both along the 'valleys', tracing the local lowest values of the reliability field. Then residue pairs like those in Fig. 2(a) can be detected by value comparison on reliability.

2.3 Phase Unwrapping Based on MBT and Reliability Map

When there are no more detectable residue pairs, we get MBT of paired residues and a reliability map of unpaired residues, including those on the borders. The constructed MBT provide explicit information about discontinuity boundaries, and the reliability map implies other undetected boundaries. Here we perform a Flood-Filling operation on the reliability map during unwrapping, which can solve such problems for implicit boundaries easily.

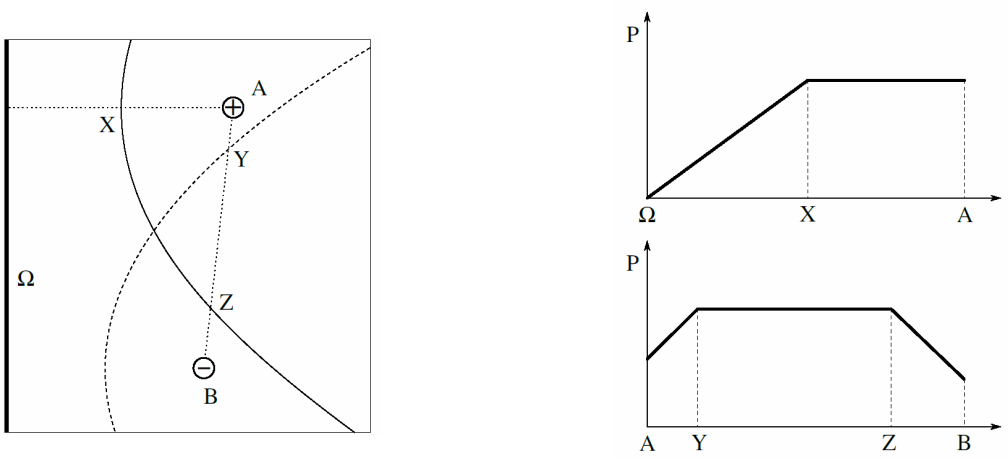

(a) Two residues with different signs near the border

(b) reliability chart for two connecting lines

Fig. 2. The connection between residues and border

The unwrapped phase can be obtained by integrating the gradient on paths from a given reference with a known absolute phase value. There are different paths between a target point and the reference, and integration paths must be consistent with the Flood-Filling. The minimal reliability on a path is taken as the reliability index of the path. The definition of this on path s is

$$P(s) = \min\{P(u,v) \mid (u,v) \in s\} \ .$$

A path of too low reliability suggests it passes through an unreliable area that may contain a phase discontinuity. So among different choices, the most reliable integration path, l, from reference point r to the target point t, should be

$$l_t = \arg\min\{P(s) \mid s : (x_r, y_r) \to (x_t, y_t)\} \ . \tag{4}$$

According to this definition, we take the maximum integration path reliability at t as its priority F, which determines the integration order during unwrapping; namely

$$F(x_t, y_t) = P(l_t) = \min\{P(u,v) \mid (u,v) \in l_t\} \ . \tag{5}$$

The priority based on path reliability provides a quantized description of the most reliable integration path, which is expected to guide the unwrapping to obtain a reliable result.

2.4 Numerical implementation

The implementation of the proposed method mainly focuses on constructing reliability maps and MBT on discrete points. There are two kinds of points, one for data sampling positions and another for potential phase discontinuity boundaries. The edges that connect the boundary points are potential discontinuity boundaries. Each boundary point is designed with attributes of reliability p_+ and p_-, total reliability p, previous neighbors' n_+ and n_-, referencing point s_+ and s_- and priority f. Each boundary edge is with quality weight q, and difference d between numbers of forwarding and reverse pair connecting lines there. If d is non-zero, the edge will be a superconductor with zero-valued q during reliability calculating and a barrier during path integration. Any sampling connecting edge might be a potential integration path. Each sampling point is with wrapped phase φ, integration priority f_i and unwrapped phase Φ, and each sampling edge is with wrapped phase gradient $\nabla\psi$, which is used in the path integration. The entire processing flow is described briefly as in Algorithm 1.

Table 1. PU based on MBT

Algorithm 1. PU based on MBT

1. detect residues;
2. initialize s_+, s_-, p_+, p_-, n_+, n_-, d;
3. repeat
4. repeat
5. solve p_+, p_- with q, d;
6. update s_+, s_-, n_+, n_-;
7. until p_+, p_- converged
8. search for dual pairs with s_+, s_-;
9. connect lines with n_+ or n_-;
10. update d;
11. until no dual pair
12. calculate $p = p_+ + p_-$;
13. search for a maximum of p map;
14. initialize f and φ;
15. repeat
16. calculate f with p;
17. until cover all points
18. repeat
19. calculate φ with $\nabla\psi$, f, d;
20. until cover all points

According to the reliability definition, p_+ and p_- at residue points are zero, and the relation between p_+ or p_- and q can be rewritten in eikonal equations as

$$\left|\Delta p_+(m,n)\right| = \left|\Delta p_-(m,n)\right| = q(m,n), \tag{6}$$

where $|\cdot|$ is the absolute value operator, and Δ refers to the difference operator. There are different ways to define the quality weight q, including constants, pseudo coherence coefficient, the inverse of maximum gradient, or derivative variance [1]. Namely,

$$q = \begin{cases} 1 & \text{constant} \\ c_{\mathrm{p}} & \text{pseudo coherence} \\ (\varepsilon + \sigma_{\Delta}^2)^{-1} & \text{derivative variance} \\ \left[\varepsilon + \max(|\Delta|)\right]^{-1} & \text{maximum gradien} \end{cases},$$

where c_{p} refers to pseudo coherence coefficient, σ_{Δ}^2 refers to derivative variance including two directions, $\max(|\Delta|)$ refers to the maximum absolute value of gradient, and ε refers to a small positive constant to avoid zero divisors. Moreover, most processing in Algorithm 1 can be designed to run in parallel. When big data blocks are divided into small blocks as individual computing units, the proposed method will achieve higher efficiency.

3 Data Experiments and Resultant Analysis

The machine that we used for the unwrapping process in the experiments was equipped with a CPU (4 cores, 2.7 GHz) and a GPU (2 multiprocessors, 384 cores, 0.71 GHz) with 2 GB device memory (1400 MHz), a 12 GB host memory (dual-channel, DDR3, 1600 MHz) and a 64-bit operating system. The proposed unwrapping method performed on a block of real InSAR phase data. The real data block came from the ROI_PAC data set [27] and had a size of 1398×622 pixels. The data contained an overall variation with serious noise at several locations, shown as in Fig. 3, and the noise produced 16212 residues. We employ the proposed method in four different forms. Including a combination of considering MBT or not and taking border potential residues or not.

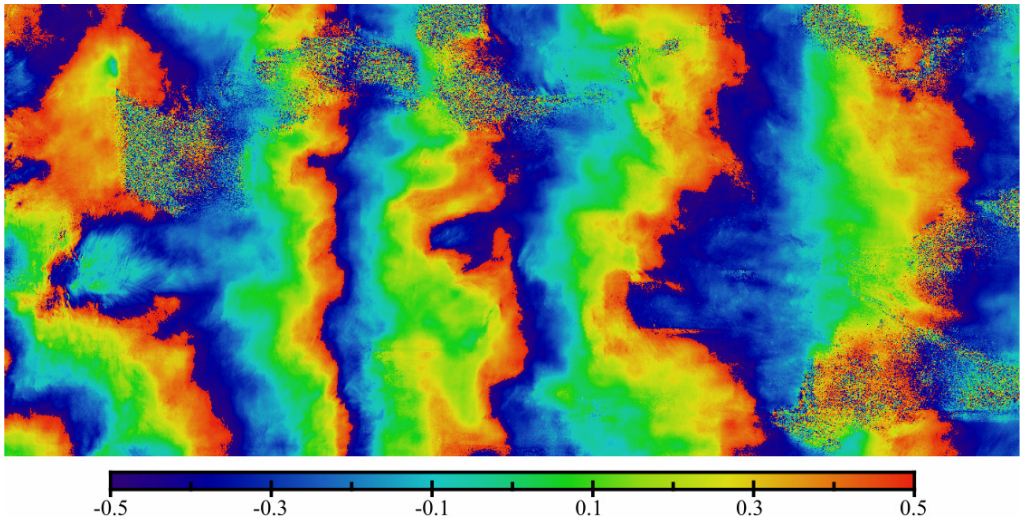

Fig. 3. Wrapped phase from real InSAR data

The processing of experimental data includes several steps. Firstly, the residue points in the data are detected by the circular integration of wrapped gradients, and then their positions and signs are marked for the following procedure. They are reference points for calculating the reliability map. Also, there are calculations of the quality map. According to the four different definitions described above, the continuous quality indicators are estimated in the horizontal and vertical directions within a fixed neighborhood window.

The next step is to calculate the reliability maps based on phase residues, which is the basis for building MBT. When using residues for reliability maps, potential residues outside the defined domain are a part worth considering. Generally, according to their positive and negative signs, the residues in the phase data domain are mostly balanced, and the proportion of the unbalanced number is tiny. For this issue, we take two strategies. One is to ignore potential residue points outside and only consider internally detectable residues. The other is to treat all points on the boundary as potential residue points.

The process was implemented according to the reliability definition, and the total reliability maps obtained without MBT are shown in Fig. 4. As shown, the residues from the nosy phase all are surrounded by areas with low values, considering border residues or not. The maximum reliability in the left column tends to escape from the domain inside, while the right one is completely enclosed. They all provide the most reliable distribution of phase region. With these maps, it is not difficult to obtain good unwrapped results in the areas with high values. However, the reliability maps without MBT cannot guarantee good results in the noise region, and the responding unwrapped results from Flood-Filling are shown in Fig. 7.

In the area far from noise, the unwrapping processing can recover the continuous phase correctly. However, in the vicinity of the noise, the continuity of the unwrapped phase values is destroyed. That is because of the Flood-Filling method without MBT. When the threshold alters, the priority path is straightforward to break through the more complicated residue point pairs. The phase differences accumulated in different directions seems grave when they meet. That is caused by the characteristic of the Flood-Filling algorithm itself.

As mentioned, the MBT are based on dual residue pairs, which are detected from positive and negative reliability maps. We calculate the reliability by labeling the influencing region of each residue point separately. The minimum reliability values within these influencing regions are derived from the corresponding residue point. The propagation of residues makes influencing regions are shown in Fig. 5 with random colors. It can be seen from the figure that in the case of considering or not considering the boundary points, the area where the residue points are dense, the influencing regions are small. In the area where the residual is sparse, relatively large regions will appear. The distribution of the influencing regions are directly related to the reliability map, and the boundary corresponds to the location with more excellent reliability. We can easily find the positive and negative residue reference with minimum reliability at any position by querying the influencing regions of different signs. According to the definition of dual residue pair, the pair detection is performed at the position of positive or negative residues.

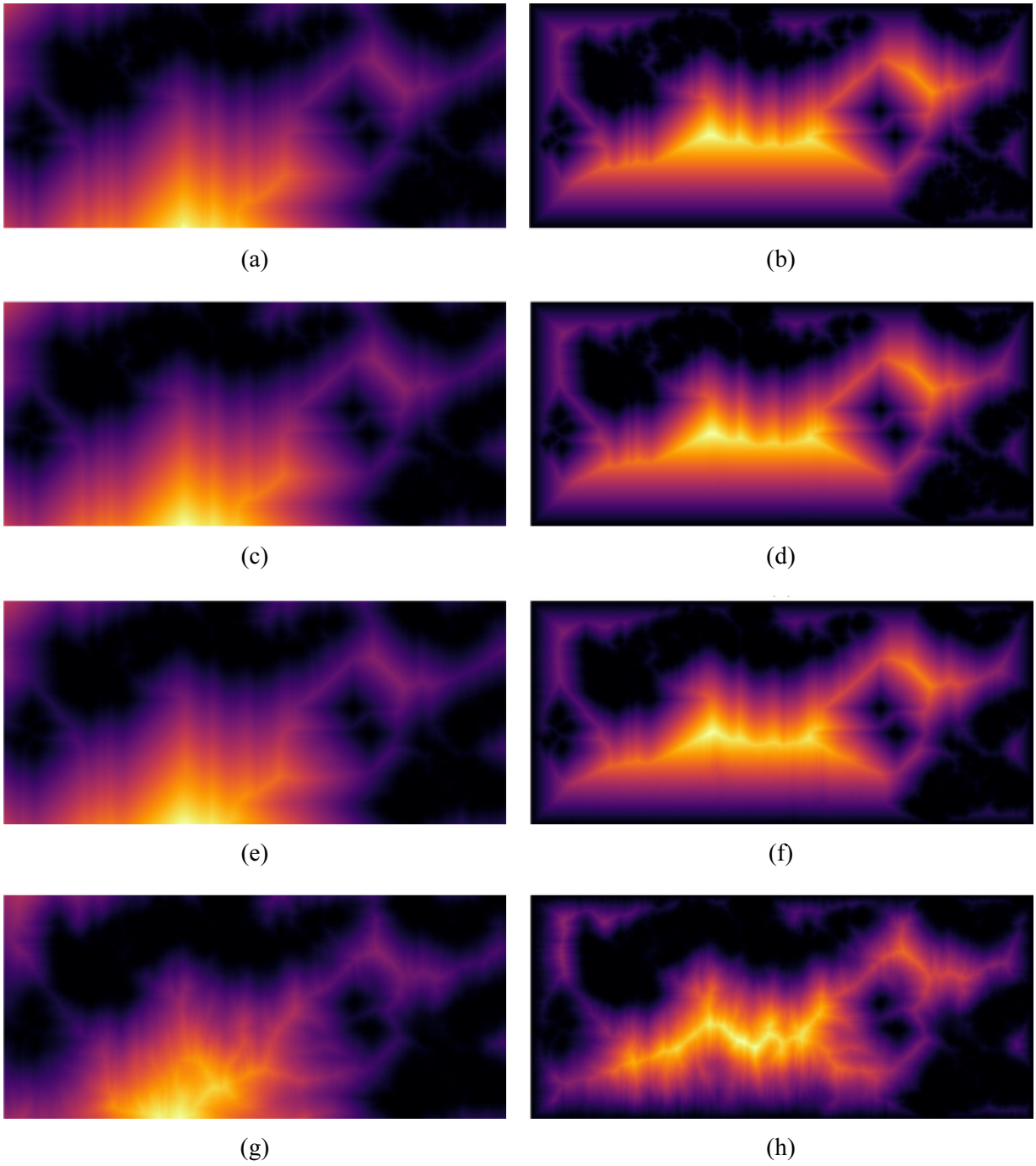

Fig. 4. Reliability maps without MBT not including border residues (left) and including (right). The top row takes the constant weights, the second takes the pseudo coherence coefficient, the third takes the inverse of derivative variance, and the bottom takes the inverse of the maximum gradient

After detecting the minimum residual point pair, the connection path is tracked according to the direction of the gradient of the reliability. Depending on the direction, specific mark values are attached to the boundaries corresponding to these link lines. The coupled residue points cannot be used as the reliability references, and the corresponding influencing regions are eliminated, and the reliability values are recalculated from the uncoupled residue points. In the calculation process, the connection lines of point pairs are superconducting. After times of dual pair detecting and expanding for MBT, we obtain the reliability maps, which ware shown in Fig. 6. With comparing Fig. 6 and Fig. 5, it is evident that coupled residue pairs change some areas with lower values in Fig. 5.

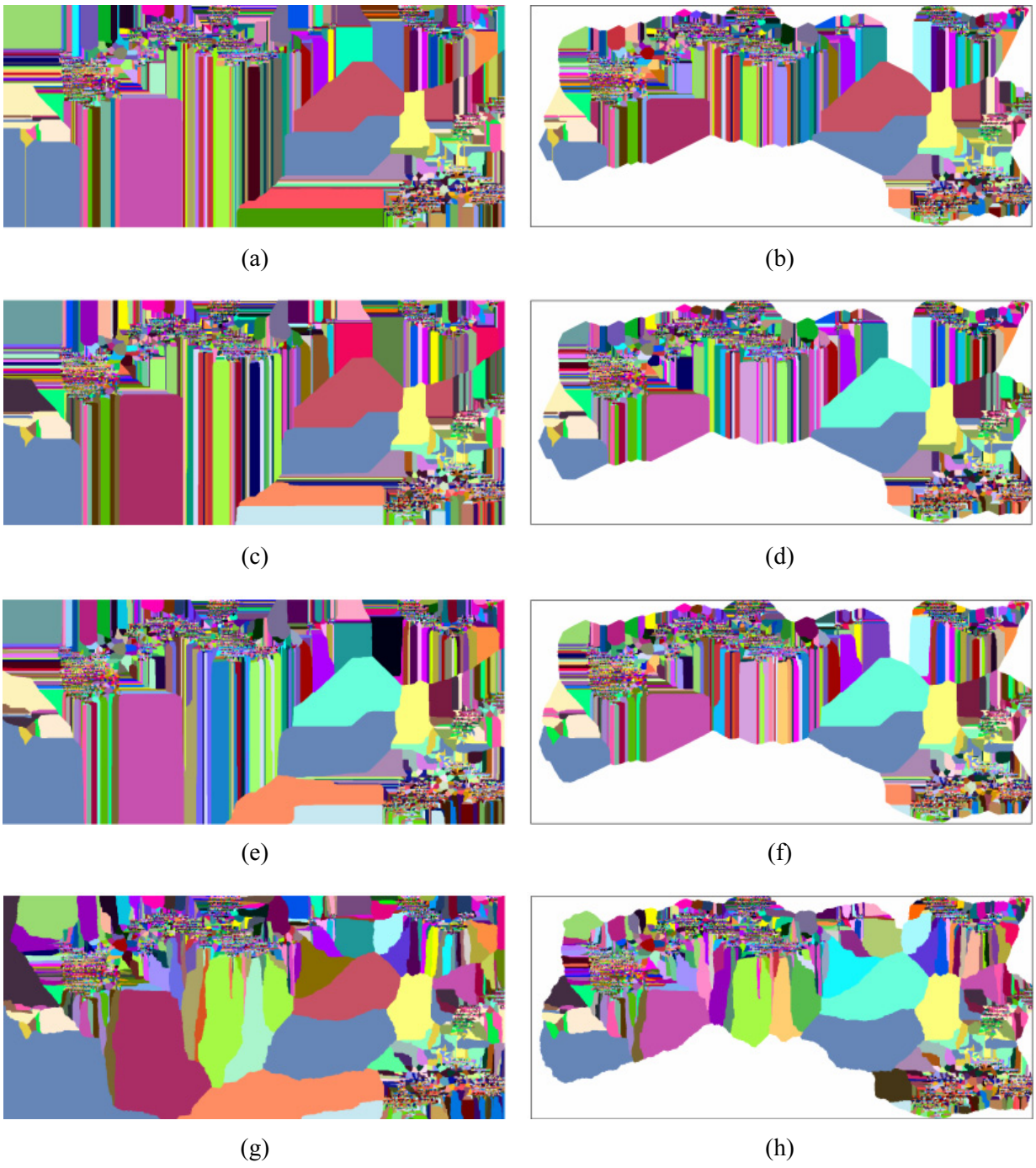

Fig. 5. The influencing regions of positive residues not including border (left) and including (right). The top row takes the constant weights, the second takes the pseudo coherence coefficient, the third takes the inverse of derivative variance, and the bottom takes the inverse of the maximum gradient

When the MBT reliability map is constructed, the smooth value distribution is more simplified, and the characteristics of different quality definitions are more visible. Constant weights still maintain the typical characteristics of geometric distance. Pseudo-correlation coefficients and inverse variance weights have quadratic characteristics, which makes pair coupling significantly different from that of constant weights during MBT construction. The local characteristics of the reliability map corresponding to the maximum gradient inverse weight are more apparent than others.

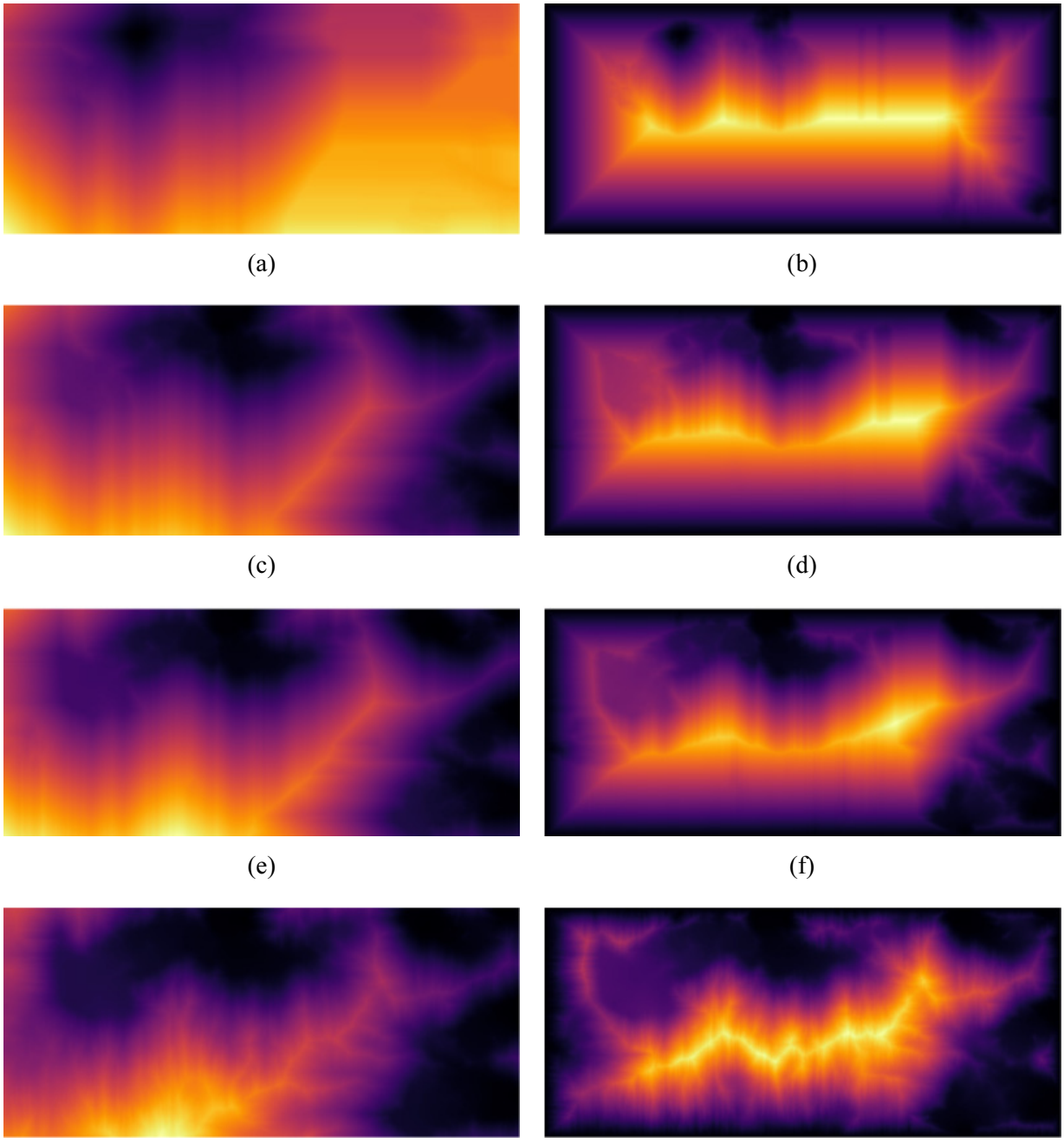

Fig. 6. Reliability maps with MBT, not including border residues (left) and including (right). The top row takes the constant weights, the second takes the pseudo coherence coefficient, the third takes the inverse of derivative variance, and the bottom takes the inverse of the maximum gradient

According to the reliability map, starting from the position with the highest reliability value to lower, using the method of the Flood-Filling and gradually lowering the reliability water level line, the order of exposure of the water surface in the defined area can be obtained. This order of priority corresponds to the order of priority of our phase expansion path integration. The reliability map in Fig. 6 has determined that the high quality and the continuous distribution at the paired residue points.

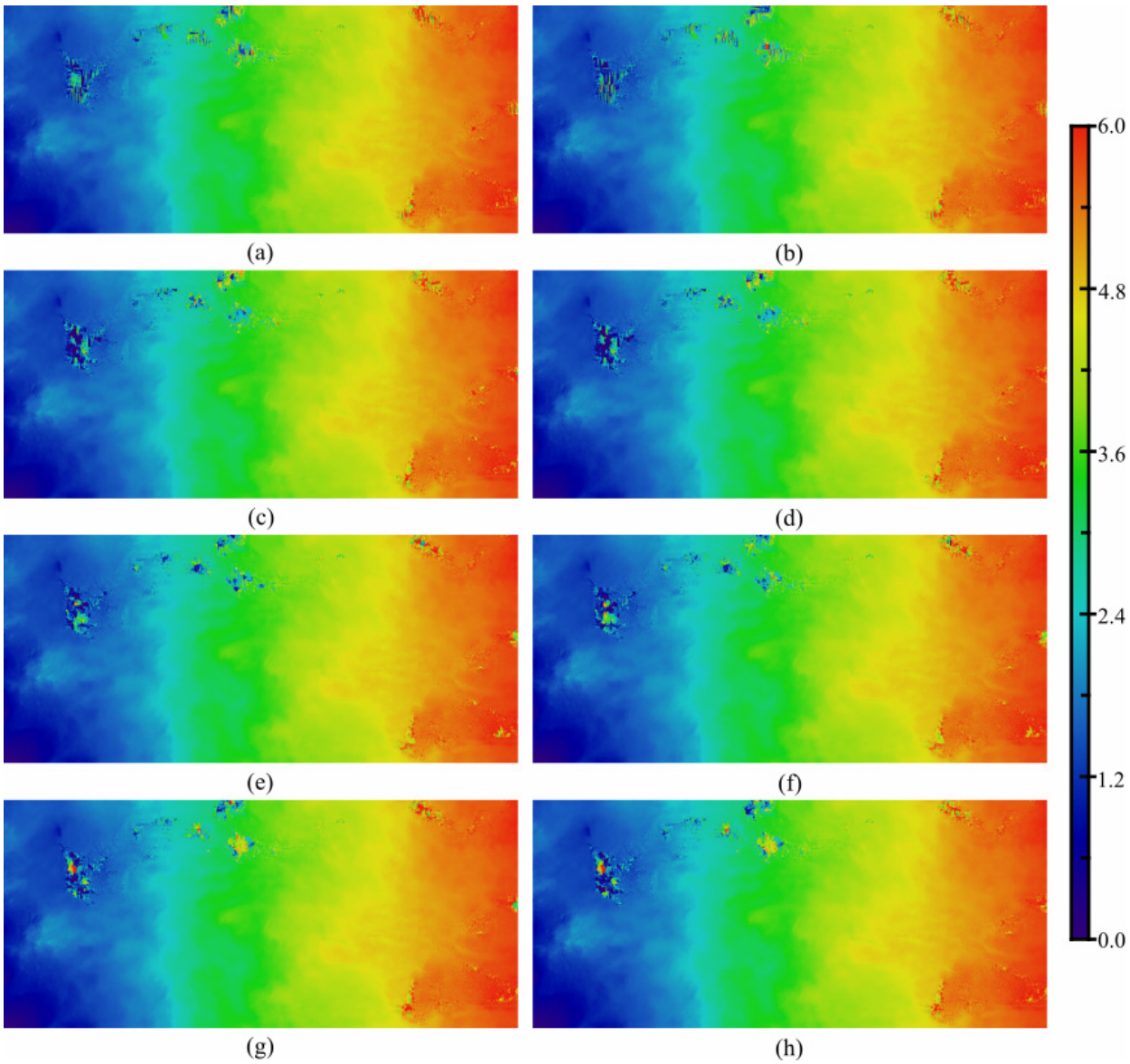

Fig. 7. Unwrapped phase from reliability maps without MBT, not including border residues (left) and including (right). The top row takes the constant weights, the second takes the pseudo coherence coefficient, the third takes the inverse of derivative variance, and the bottom takes the inverse of the maximum gradient

With the reliability maps and MBT, unwrapped results obtained from Flood-Filling are shown in (a~h) of Fig. 8. Most of the results are normal except that result (a) are discontinuous on the top border. Compared to Fig. 7, the results with MBT do better in nosy areas with smoother unwrapped phase or less discontinuity.

That shows the superiority of MBT over Flood-Filling strategy in identifying discontinuous boundaries and maintaining phase continuity. The wrong unwrapping phase in the center area of the upper boundary in figure (a) confirms that the potential residue points outside the boundary may be considered to cause incorrect coupling. This problem is suppressed to some extent when other non-constant weights are used.

For comparison, other traditional phase unwrapping methods, including Goldstein's branch-cut and SNAPHU, and our proposed method were applied to the same data. The result from Goldstein's is shown in (i) of Fig. 8, and the result from SNAPHU is shown in (j). From a visual comparison, it is clear that all methods work well in good-quality areas of the wrapped data. However, Goldstein's result is with some distinct holes in the noisy areas, which almost disappear in SNAPHU's result. The different principles of the two methods determined this difference. The Goldstein's method directly performs residue point

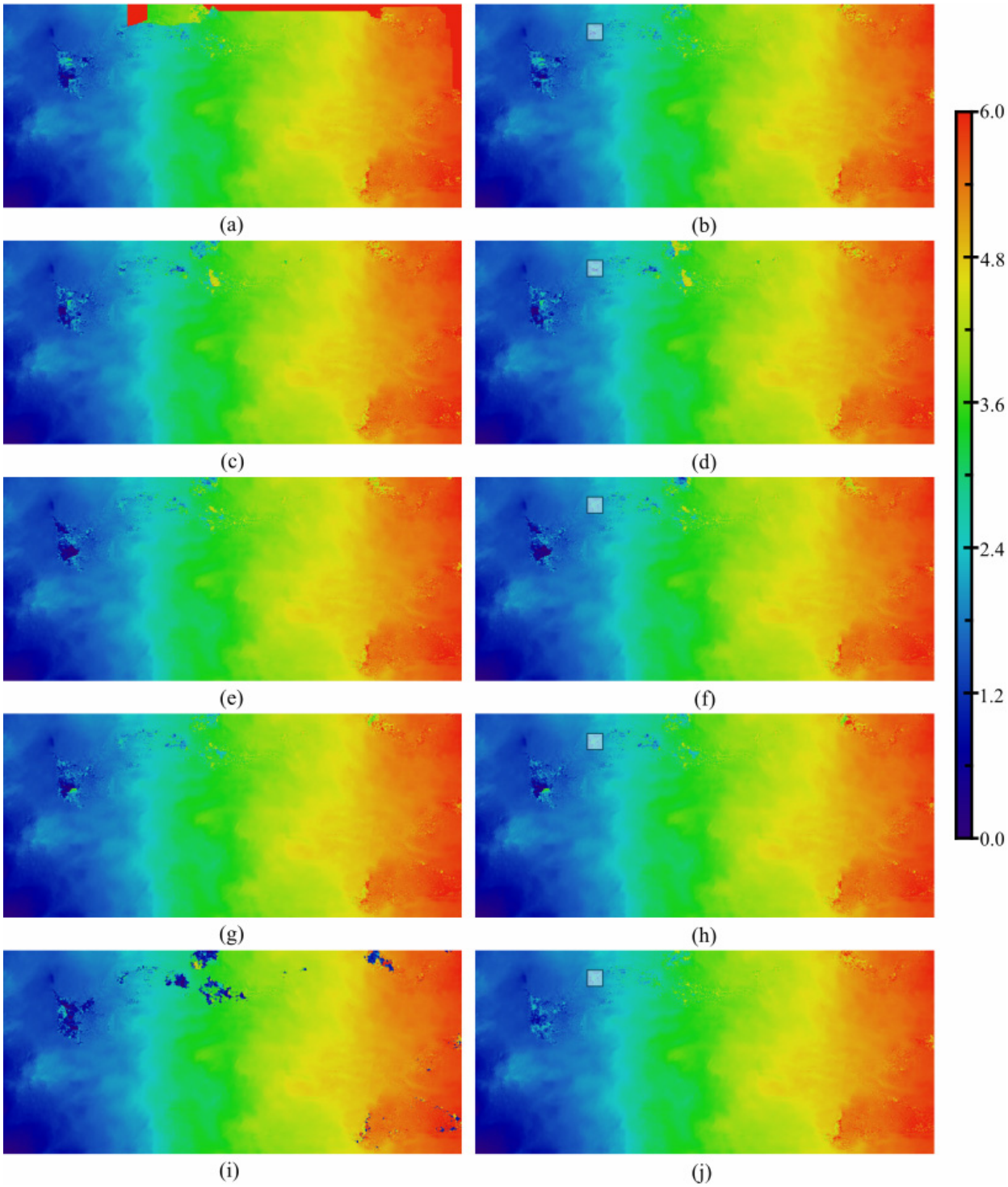

Fig. 8. Unwrapped phase form reliability maps with MBT, Goldstein's, and SNAPHU. The top row takes the constant weights, and the second takes the pseudo coherence coefficient, and the third takes the inverse of derivative variance, and the forth takes the inverse of the maximum gradient, and the bottom is from Goldstein's (i) and SNAPHU (j)

coupling based on the random nearest distance, which is very tolerant of discontinuous boundaries or even closed areas caused by errors, although the algorithm is efficient and straightforward. The SNAPHU method only has more complicated weight calculation and network optimization algorithms, and it obtains smoother results, and it also pays more time cost. The results from the proposed method look a little different in the noisy areas, and they are all better than Goldstein's except (a).

For further comparison, we extracted some local detailed discontinuity boundaries in a marked noisy area from (b), (d), (f), (h), (j) of Fig. 8. The red points refer to positive residues, and green points refer to negative ones. The black connecting lines refer to boundaries from MBT, and the blue connecting lines from Flood-Filling, and red lines from the change between MBT and Flood-Filling. It can be found in the figure that MBT in the proposed method can achieve most of the residue point coupling, and only a small part needs to be achieved by Flood-Filling. There are no red marks, and its probability is very low in actual statistics. Only when the constant weights are used in the proposed method, the connection of the residue points by the Flood-Filling method appears in the investigating area. When using pseudo-correlation coefficients, the inverse of gradient variances, and maximum gradients, the MBT of the proposed method is competent for the task of coupling all residue points. Compared with MBT, the Flood-Filling method does not guarantee the optimal connection or the shortest connection. We can find that the SNAPHU method does not guarantee the minimum L^0 norm, although its design principle is derived from the principle of the minimum norm. The residue points tracked by MBT in experimental data have the characteristics of the shortest connection. Although the constant weight definition will affect the point pair coupling result, the length of some of the lines in (b) is slightly longer. In general, the MBT method can achieve the coupling of residue point pairs and phase discontinuous boundary tracking.

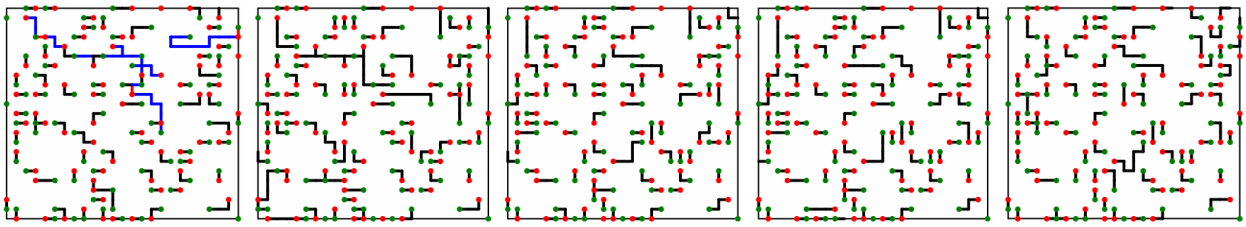

Fig. 9. Local detailed discontinuity boundaries from MBT (in black) and Flood-Filling (in blue) and the change from MBT to Flood-Filling (in red) of (b, d, f, h), and from SNAPHU (j) in Fig. 8. The red points refer to positive residues and the green point refer to negative residues

Statistical indexes of all the unwrapped results, including the L^0 norm and the L^1 norm of phase discontinuity boundaries and running times, were calculated for quantitative analysis. Discontinuity length and running time indices are listed in Table 2. It is apparent that among the discontinuity length indices for the unwrapped results, the L^0 and the L^1 norm lengths for SNAPHU are the same, meaning that there are only single-cycle jumps in its unwrapped phase, which explains the smooth of its unwrapping results. The index value of the Goldstein's method is not ideal, although its running time is the shortest. In the experimental results of the proposed method, the index using non-constant weights is better than the constant weight, and the index using the MBT scheme is better than the result without MBT. Our maximum gradient weights with MBT and border residues bring about the shortest L^0 discontinuity length according to the indices, and inverse derivative variance weights with MBT and border residues provide smaller discontinuity length on the L^1 norm than others. Although there are multiple-cycle jumps, which would sharpen their discontinuity visualization in Fig. 8, the results from the proposed verified that our method is eligible to be a reliable unwrapping option.

For the unwrapping processing of large-scale data, the time cost is one of the critical factors when choosing the unwrapping method. Considering the increasing need for high efficiency, we also take the run times for another comparison. Goldstein's method runs with the shortest time of 0.221s, and SNAPHU takes the longest time 18.916s. All the times cost in performing the proposed method are not more than 10s in parallel mode. No matter which weight is used, the number of iterations to build the MBT is about ten times. The time complexity of the algorithm is insensitive to weights and is stable. The proposed method is significantly more efficient than SNAPHU, although the MBT construction and renewal of reliability maps also include iterative operations.

Table 2. Discontinuity lengths, iteration numbers and running times of PU processing

Weight	Coupling	Border	L^0 norm (pix)	L^1 norm (pix)	Iteration	Time (sec)
Constant	False	False	24841	31305	-	3.621
		True	25475	33516	-	4.060
	True	False	14058	24010	9	5.419
		True	12570	12845	10	4.917
Pseudo coherence	False	False	20343	23598	-	4.212
		True	20356	23582	-	4.495
	True	False	13585	14102	10	7.454
		True	13678	14208	10	5.796
Derivative variance	False	False	19262	22298	-	4.295
		True	19309	22357	-	4.524
	True	False	12874	13309	11	8.707
		True	12918	13330	11	6.047
Maximum gradient	False	False	19350	22711	-	4.317
		True	19442	22769	-	4.451
	True	False	12918	**12799**	11	8.158
		True	**12561**	12923	11	6.339
Goldstein's			17351	30260	-	**0.221**
SNAPHU			12997	12997	-	18.916

4 Conclusion

We present a novel PU method based on MBT in this paper. First, we take phase residue points as references and take data quality-related indices in the horizontal and vertical directions were as weights. The reliability was evaluated by solving of eikonal equations. During the building of the reliability map, local minimum reliability residue pairs were detected iteratively for MBT that denote phase discontinuity boundaries explicitly. The other discontinuity boundaries undetectable were implied in a priority map derived from implementing Flood-Filling to the reliability map. The result was produced by path integration based on the priority map and MBT. All these procedures could run in parallel mode, which significantly improves the processing efficiency. We implemented a novel method on the GPU device platform and performed real data experiments and resultant comparison and analysis. Data analysis shows that the proposed unwrapping method can obtain more reliable unwrapping results by using appropriate weights and has higher processing efficiency. We hope the novel PU method could provide a robust and efficient option for large-scale PU problems.

However, we find that the proposed method still has limitations. For example, the Flood-Filling strategy used in the path integration sometimes fails to make full use of the priority information provided by the reliability map, resulting in locally unstable unwrapping results. Besides, the proposed method is mainly aimed at large-scale continuous and locally discontinuous interference phase data. In some extreme cases, the interference data may be segmented by complicated noise to be sufficiently continuous. In this situation, we must consider the optimal connection between locally continuous segmentations. Therefore, our further research would focus on the robust unwrapping scheme of uncoupled residue points and the connection of locally continuous segmentations.

References

[1] D. C. Ghiglia, M. D. Pritt, Two-dimensional phase unwrapping: theory, algorithms, and software, Wiley-Interscience, Wiley, 1998.

[2] R. M. Goldstein, H. A. Zebker, C. L, Werner, Satellite radar interferometry: Two dimensional phase unwrapping, Radio Science 23 (4)(1988) 713-720.

[3] H. Yu, H. Lee, A convex hull algorithm based fast large-scale two-dimensional phase unwrapping method, in Proc: In 2017 IEEE International Geoscience and Remote Sensing Symposium (IGARSS), 2017.

[4] H. Yu, Y. Lan, J. Xu, D. An, H. Lee, Large-Scale L0-Norm and L1-Norm 2-D Phase Unwrapping, IEEE Transactions on Geoscience and Remote Sensing 55(8)(2017) 4712-4728.

[5] H. Yu, Y. Zhou, S. S. Ivey, Y. Lan, Large-Scale Multibaseline Phase Unwrapping: Interferogram Segmentation Based on Multibaseline Envelope-Sparsity Theorem, IEEE Transactions on Geoscience and Remote Sensing 57(11)(2019) 9308-9322.

[6] X. Xie, Q. Zeng, Multi-baseline extended particle filtering phase unwrapping algorithm based on amended matrix pencil model and quantized path-following strategy, Journal of Systems Engineering and Electronics 30(1)(2019) 78-84.

[7] Q. Huang, H. Zhou, S. Dong, S. Xu, Parallel Branch-Cut Algorithm Based on Simulated Annealing for Large-Scale Phase Unwrapping, IEEE Transactions on Geoscience and Remote Sensing 53(7)(2015) 3833-3846.

[8] J. Gao, J. Li, L. Shi, Two-dimensional Phase Unwrapping Method Using Cost Function of L0 Norm, in Proc: IOP Conference Series: Earth and Environmental Science, 2017.

[9] X. Wang, S. Fang, X. Zhu, Weighted least-squares phase unwrapping algorithm based on a non-interfering image of an object, Applied Optics 56(15)(2017) 4543.

[10] M. Wang, C. Zhou, S. Si, X.-L. Li, Z. Lei, Y.-J. Li, Robust wrapping-free phase retrieval method based on weighted least squares method, Optics & Lasers in Engineering 97(2017) 34-40.

[11] D. Feng, N. Wu, B. Liu, A Region-growing Phase Unwrapping Approach Based on Local Frequency Estimation for Interferometric SAR, in Proc: 2006 8th international Conference on Signal Processing, 2006.

[12] H. Zhong, S. Zhang, J. Tang, Path Following Algorithm for Phase Unwrapping Based on Priority Queue and Quantized Quality Map, in Proc: 2009 International Conference on Computational Intelligence and Software Engineering, 2009.

[13] M. Zhao, K. Qian, Quality-guided phase unwrapping implementation: an improved indexed interwoven linked list, Applied Optics 53(16)(2014) 3492-3500.

[14] H. Zhong, J. Tang, S. Zhang, M. Chen, An Improved Quality Guided Phase-Unwrapping Algorithm Based on Priority Queue, IEEE Geoscience and Remote Sensing Letters 8(2)(2011)364-368.

[15] H. Zhong, J. Tang, S. Zhang, X. Zhang, A Quality-Guided and Local Minimum Discontinuity Based Phase Unwrapping Algorithm for InSAR/InSAS Interferograms, IEEE Geoscience and Remote Sensing Letters 11(1)(2014) 215-219.

[16] G. Liu, R. Wang, Y. Deng, R. Chen, Y. Shao, Z. Yuan, A New Quality Map for 2-D Phase Unwrapping Based on Gray Level Co-Occurrence Matrix, IEEE Geoscience and Remote Sensing Letters 11(2)(2014) 444-448.

[17] J. Dong, Z. Zhuo, J. Li, Y. He, A new phase image reconstruction method using Markov random fields, in Proc: IEEE/ACIS 16th International Conference on Computer and Information Science, 2017.

[18] T. Chen, Y. Ding, R. Pang, C. Gong, D. Xu, H. Zhang, B. Chen, Phase Unwrap Using Nonlinear Kalman Filtering for SAR Systems, in Proc: IEEE International Geoscience and Remote Sensing Symposium, 2019.

[19] K. Chen, J. Xi, L. Song, Y. Yu, An object image edge detection based quality-guided phase unwrapping approach for fast three-dimensional measurement, in Proc: IEEE International Conference on Advanced Intelligent Mechatronics, 2013.

[20] Y. Zhang, Z. Xing, A Hybrid Phase Unwrapping Algorithm Based on Quality-Guided and Surface-Fitting, in Proc: IEEE International Workshop on Electromagnetics: Applications and Student Innovation Competition, 2018.

[21] A. Karsa, K. Shmueli, SEGUE: A Speedy rEgion-Growing Algorithm for Unwrapping Estimated Phase, in Proc: IEEE Transactions on Medical Imaging, 2019.

[22] F. Xiao, J. Wu, L. Zhang, X. Li, A new method about placement of the branch cut in two-dimensional phase unwrapping, in Proc: Asian and Pacific Conference on Synthetic Aperture Radar 2007.

[23] J. Gao, Reliability-Map-Guided Phase Unwrapping Method, IEEE Geoscience and Remote Sensing Letters 13 (5)(2016) 716-720.

[24] M. Costantini, A novel phase unwrapping method based on network programming, IEEE Transactions on Geoscience and Remote Sensing 36(3)(1998) 813-821.

[25] C. W. Chen, H. A. Zebker, Two-dimensional phase unwrapping with statistical models for nonlinear optimization, in Proc: IEEE 2000 International Geoscience and Remote Sensing Symposium, 2000.

[26] R. Li, X. Lv, Y. Yun, A Network-Optimization-Based L1-Norm Sparse 2-D Phase Unwrapping Method for Persistent Scatterer Interferometry, IEEE Geoscience and Remote Sensing Letters 15(5)(2018) 709-713.

[27] P. A. Rosen, S. Henley, G. Peltzer, M. Simons, Updated Repeat Orbit Interferometry Package Released, Eos Transactions American Geophysical Union 85(5)(2013) 47-47.